PRAMANA
— journal of
physics

Vol. 62, No. 5
May 2004
pp. 1073–1082

Triple differential cross-sections for near threshold $(e, 2e)$ process for hydrogen

M K SRIVASTAVA[1] and R K CHAUHAN[2]
[1]Institute Instrumentation Centre, Indian Institute of Technology, Roorkee 247 667, India
[2]Department of Physics, Indian Institute of Technology, Roorkee 247 667, India
E-mail: mksrific@iitr.ernet.in; rajkrdph@iitr.ernet.in

MS received 14 November 2003; revised 27 January 2004; accepted 13 March 2004

Abstract. The triple differential cross-sections for ionization of hydrogen at incident energies in the range 17.6 eV to 13.7 eV are calculated in the distorted-wave Born approximation in the equal energy sharing and $\vartheta_{ab} = 180^\circ$ kinematics. It is found that a maximum in the cross-section, as was observed in the case of helium under similar conditions is also found here at excess energy $E_{\rm ex} \leq 1.0$ eV. This 'maximum' becomes more pronounced as $E_{\rm ex}$ decreases indicating dominance of short range e–e correlations at these low energies. The angular distribution of the singlet and triplet partial waves and the asymmetry parameter have been analysed.

Keywords. Triple differential cross-section; very close to threshold; singlet/triplet contribution; asymmetry parameter.

PACS No. 34.80.Dp

1. Introduction

Low energy $(e, 2e)$ experiments for hydrogen and helium [1–3] and for neon, argon, krypton and xenon [4,5] have shown that the triple differential cross-sections (TDCS) are highly dependent on target-dependent short range correlations and lead to different angular distributions even though at asymptotic separations the long-range interactions in the final state are essentially identical and target independent. These experiments have prompted several studies to understand the dynamics of ionization close to threshold. The calculations were done with emphasis on asymptotically correct three-body boundary conditions [6–11], in distorted-wave Born approximation (DWBA) [12–19], convergent close-coupling (CCC) approximation [20–22], exterior complex scaling method [23,24] and a quantal-semiclassical treatment [25,26]. These studies have tried to analyse the roles played by exchange contribution [13–15], capture process (if possible) in which the projectile electron is captured by the target and the two target electrons are ejected [13,14], post-collision interaction [14,15] and target polarization [18,19]. The role of Coulomb

three-body effects in the incident and final channels has recently been analysed by Roder *et al* [27].

Let us consider equal energy sharing results in which the two electrons in the final state are detected in opposite directions ($\vartheta_{ab} = 180°$). The results in this geometry are least affected by post-collision interaction and the use of effective charges is quite appropriate. One of the striking features in the angular distribution of TDCS in this kinematics in the experiments of Selles *et al* [1,4] and Schlemmer *et al* [2] was a qualitative similarity in the results for hydrogen and neon. The TDCS decreases with increasing scattering angle ϑ_a reaching to a minimum value at $\vartheta_a = 90°$. In the case of helium, the TDCS first decreases, then increases and reaches to a maximum at $\vartheta_a = 90°$. It is found to show a little more structure in the case of argon, krypton and xenon. The structure in the angular distribution of TDCS becomes more pronounced as the excess energy $E_{\rm ex}$ (incident energy E_i minus ionization energy I) decreases and the cross-sections are calculated closer to the ionization threshold. Away from the threshold as $E_{\rm ex}$ increases, the angular distributions of the TDCS for all the cases become similar and qualitatively identical to the results for hydrogen. At these energies the effect of short range correlations is no longer dominant. The energy region very close to the threshold is therefore of particular interest.

The studies for hydrogen which is the simplest target at $E_{\rm ex}$ very close ($\leq$1.0 eV) to the threshold have been done by Roder *et al* [3] ($E_{\rm ex} = 1.0$ eV) and Pan and Starace [13] ($E_{\rm ex} = 0.5$ eV) using DWBA and by Deb and Crothers [26] ($E_{\rm ex} = 1.0$ eV, 0.5 eV and 0.3 eV) using a quantal-semiclassical treatment. Pan and Starace found a maximum in the angular distribution of TDCS at $\vartheta_a = 90°$ reminiscent of the distribution for helium. Roder *et al* [3] also observed a qualitative change in the angular distribution: the bowl shape at $\vartheta_a = 90°$ flattens out. The CCC results of Bray *et al* [20] predicted a small local maximum at $E_{\rm ex} = 1.0$ eV. This partially confirmed the results of Pan and Starace [13]. However, Deb and Crothers found no such maximum even at $E_{\rm ex} = 0.3$ eV. In the latter case the distribution was as observed at higher values of $E_{\rm ex}$. We have studied the angular distribution of TDCS for hydrogen in the energy region down to $E_{\rm ex} = 0.1$ eV in the equal energy sharing, $\vartheta_{ab} = 180°$ kinematics. There are, however, no experimental results for $E_{\rm ex} < 1.0$ eV. The calculation has been done in the distorted-wave Born approximation. In the next section we outline its details. The results are presented, compared with available experimental data and discussed in §3. Section 4 contains the conclusions.

2. Calculation

The TDCS for the ionization of hydrogen by unpolarized electrons with energy E_i (momentum $\vec{k}_i$) can be defined in terms of direct amplitude f and exchange amplitude g as follows:

$$\frac{{\rm d}^3\sigma}{{\rm d}E_b {\rm d}\Omega_a {\rm d}\Omega_b} = (2\pi)^4 \, \frac{k_a k_b}{k_i} \left(\frac{1}{4} \left| f + g \right|^2 + \frac{3}{4} \left| f - g \right|^2 \right), \qquad (1)$$

where

$$f = \langle \chi_a^{(-)}(\vec{r}_0)\, \chi_b^{(-)}(\vec{r}_1)\, |V - U_i|\, \phi_i(\vec{r}_1)\, \chi_i^{(+)}(\vec{r}_0) \rangle, \tag{2}$$

$$g = \langle \chi_a^{(-)}(\vec{r}_1)\, \chi_b^{(-)}(\vec{r}_0)\, |V - U_i|\, \phi_i(\vec{r}_1)\, \chi_i^{(+)}(\vec{r}_0) \rangle, \tag{3}$$

$$V = \frac{1}{r_{01}} - \frac{1}{r_0}. \tag{4}$$

Here $\chi_a^{(-)}$ and $\chi_b^{(-)}$ are final-state distorted waves which are obtained as eigenfunctions of the distorting potential U_a and U_b, and $\vec{k}_a$ and $\vec{k}_b$ are momenta of the two electrons in the final state. The distorted wave $\chi_i^{(+)}$ for the incident electron is an eigenfunction of the initial-state distorting potential U_i and ϕ_i is the hydrogen ground state wave function .

The initial-state distorting potential U_i is the sum of static potential $U_{\rm st}$ felt by the electron, semiclassical local exchange potential $U_{\rm exch}$ of Furness–McCarthy [28] as modified by Gianturco and Scialla [29] for low energies and dipole polarization potential $U_{\rm pol}$ proposed by Hara [30]. These are given by

$$U_{\rm st}(r) = -\left(1 + \frac{1}{r}\right) \exp(-2r), \tag{5}$$

$$U_{\rm exch}(r) = \frac{1}{2}\left[E_i - U_{\rm st} + \frac{3}{10}\{3\pi^2\rho(r)\}^{2/3}\right] - \frac{1}{2}\left\{\left[E_i - U_{\rm st} + \frac{3}{10}\left\{3\pi^2\rho(r)\right\}^{2/3}\right]^2 + 4\pi\rho(r)\right\}^{1/2}, \tag{6}$$

$$U_{\rm pol}(r) = -\frac{\alpha r^2}{(r^2 + d^2)^3}, \quad \alpha = 4.5, \quad d = 1.6. \tag{7}$$

The final-state electron–electron interaction is incorporated through the use of an effective charge model. This is quite appropriate in the present geometry as the interactions between all the particles in the final state are radial. The asymptotic effective charges Z_a and Z_b for equal energy final state and $\vartheta_{ab} = 180^\circ$ are given by

$$Z_a = Z_b = 1 - 1/4 = 3/4. \tag{8}$$

This choice of effective charges satisfies the Rudge condition [31] but differs from the effective charges used by Jones *et al* [14]. The distorting potentials U_a and U_b should satisfy the limiting conditions

$$U_a(r) = U_b(r) \to \begin{cases} -\frac{1}{r} & \text{as} \quad r \to 0 \\ -\frac{Z_a}{r} & \text{as} \quad r \to \infty \end{cases}. \tag{9}$$

This is achieved by defining U_a and U_b as

$$U_a(r) = U_b(r) = -\frac{Z_a}{r} + (1 - Z_a)\, U_{\rm st}(r). \tag{10}$$

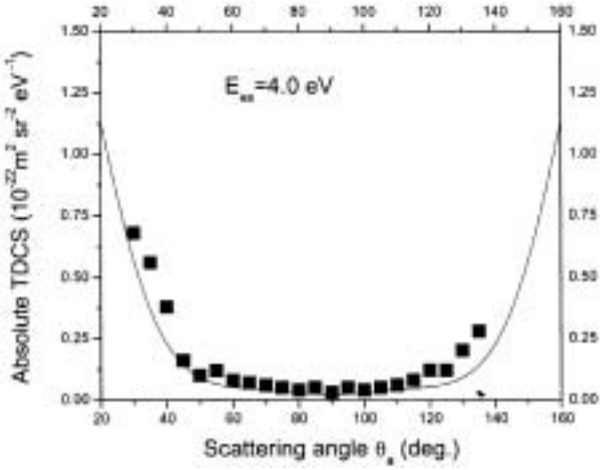

Figure 1. TDCS in units of 10^{-22} m^2 sr^{-2} eV^{-1} for electron impact ionization of hydrogen in equal energy sharing and $\vartheta_{ab} = 180^\circ$ kinematics as a function of scattering angle ϑ_a at $E_{\rm ex} = 4.0$ eV. Present results are compared with the absolute experimental data of Roder *et al* [3].

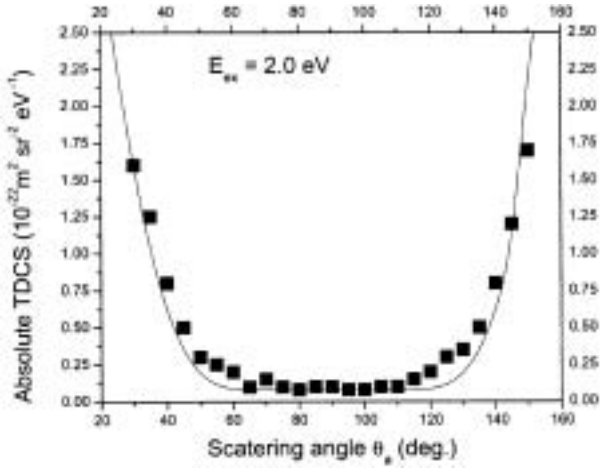

Figure 2. Same as figure 1 but at $E_{\rm ex} = 2.0$ eV. Present theoretical results have been multiplied by a factor of 2.

The distorted wave $\chi_b^{(-)}(\vec{r}_1)$ (and $\chi_a^{(-)}(\vec{r}_1)$ in the exchange amplitude) has been orthogonalised to the initial state wave function $\phi_i(\vec{r}_1)$ by Schmidt's procedure. The distorting potential U_i in the matrix elements (eqs (2) and (3)) therefore does not contribute.

The scattering amplitudes f and g are obtained by the usual partial wave expansion up to l_a, $l_b \leq 6$, $l_i \leq 12$ following the procedure of Gupta and Srivastava [18]. The contribution of higher partial waves is very small at the energies considered here (<2% at $E_{\rm ex} = 1.0$ eV and <0.1% at $E_{\rm ex} = 0.1$ eV).

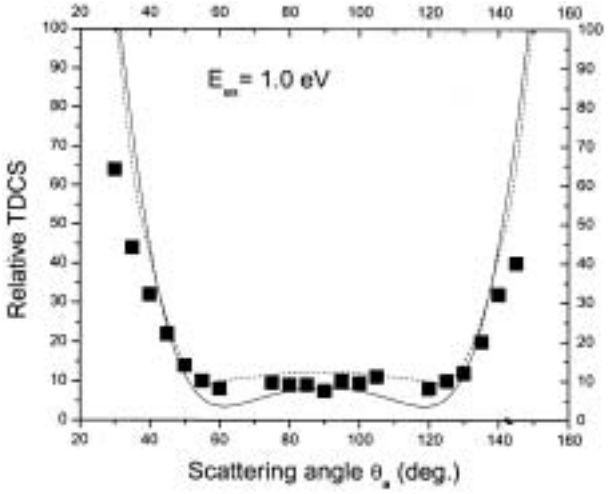

Figure 3. Present TDCS (—) along with CCC results of Bray *et al* [20] (- - -) at $E_{\rm ex} = 1.0$ eV are compared with relative experimental data of Roder *et al* [3]. All the results have been normalized to 23 at $\vartheta_a = 45°$.

3. Results

We have obtained TDCS at $E_{\rm ex} = 4.0$, 2.0, 1.0, 0.5, 0.2 and 0.1 eV. Figures 1–3 show our results at $E_{\rm el} = 4.0$, 2.0 and 1.0 eV. They are compared with the available absolute experimental data of Roder *et al* [3] at $E_{\rm ex} = 4.0$ and 2.0 eV and their relative data at $E_{\rm ex} = 1.0$ eV. The error bars on the absolute measurements are $\pm 35\%$ at $E_{\rm ex} = 2.0$ eV and $\pm 40\%$ at $E_{\rm ex} = 4.0$ eV. The present calculation is able to reproduce the angular distribution of TDCS fairly accurately. At $E_{\rm ex} = 1.0$ eV, the angular distribution around $\vartheta_a = 90°$ becomes flatter. The present results as well as the CCC results of Bray *et al* [20] show the emergence of a small maximum as in the case of helium.

We now consider the results at energies very close to threshold. Figure 4 shows that at $E_{\rm ex} = 1.0$ eV and lower values, a maximum at 90° appears. The value of the maximum TDCS at $\vartheta_a = 90°$ increases with decreasing $E_{\rm ex}$. It also becomes more prominent in the sense that the ratio of the maximum to minimum increases from about 2.5 at $E_{\rm ex} = 1.0$ eV to about 7.5 at $E_{\rm ex} = 0.1$ eV. Figure 5 shows the results around the maximum in greater detail. The incorporation of the polarization potential in the initial channel does not affect the results very much.

Let us now analyse the angular distribution of triplet and singlet cross-sections which lead to this feature (figures 6 and 7).

$$\left(\frac{{\rm d}^3\sigma}{{\rm d}E_b {\rm d}\Omega_c {\rm d}\Omega_b}\right)_T = (2\pi)^4 \, \frac{k_a k_b}{k_0} \, |f - g|^2 \,, \tag{11}$$

$$\left(\frac{{\rm d}^3\sigma}{{\rm d}E_b {\rm d}\Omega_c {\rm d}\Omega_b}\right)_S = (2\pi)^4 \, \frac{k_a k_b}{k_0} \, |f + g|^2 \,. \tag{12}$$

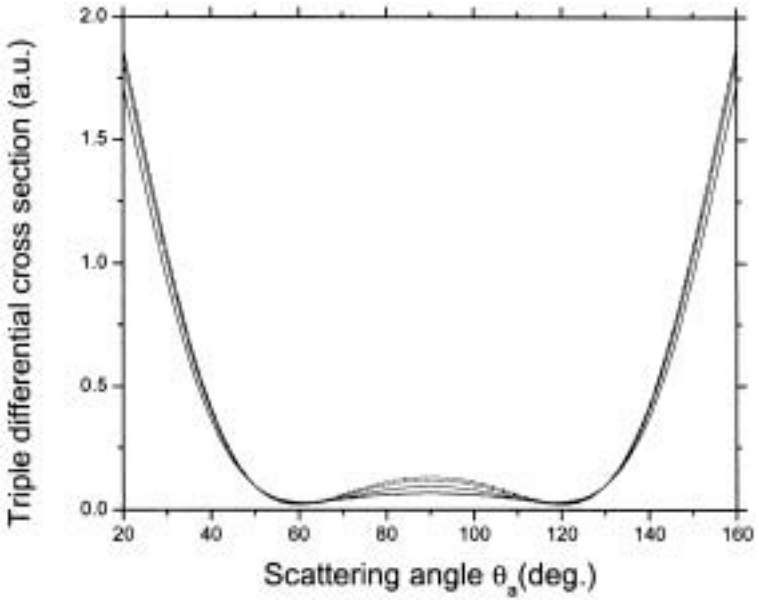

Figure 4. TDCS for electron impact ionization of hydrogen in equal energy sharing and $\vartheta_{ab} = 180^\circ$ kinematics as a function of scattering angle ϑ_a at various values of excess energy E_{ex}. Results: $E_{ex} = 0.1$ eV (- · - · · -), $E_{ex} = 0.2$ eV (- - -), $E_{ex} = 0.5$ eV (· · ·), $E_{ex} = 1.0$ eV (—).

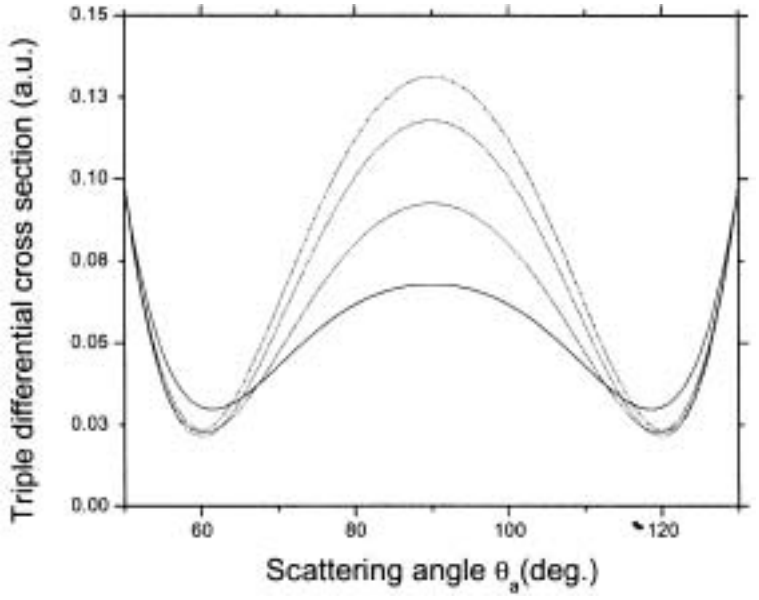

Figure 5. Same as figure 4, but for ϑ_a varying from 50° to 130°.

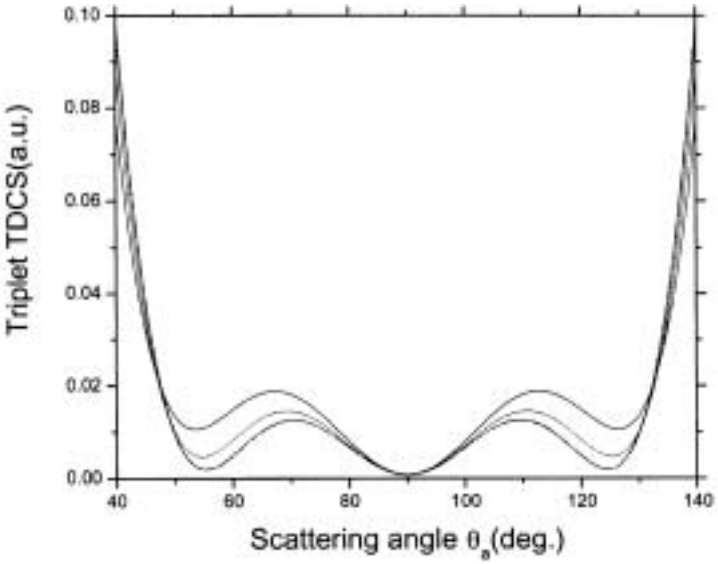

Figure 6. Triplet TDCS for electron impact ionization of hydrogen in equal energy sharing and $\vartheta_{ab} = 180^\circ$ kinematics as a function of scattering angle ϑ_a at various values of excess energy $E_{\rm ex}$. Results: $E_{\rm ex} = 0.1$ eV (- ·· - ·· -), $E_{\rm ex} = 0.2$ eV (- - -), $E_{\rm ex} = 0.5$ eV (···), $E_{\rm ex} = 1.0$ eV (—).

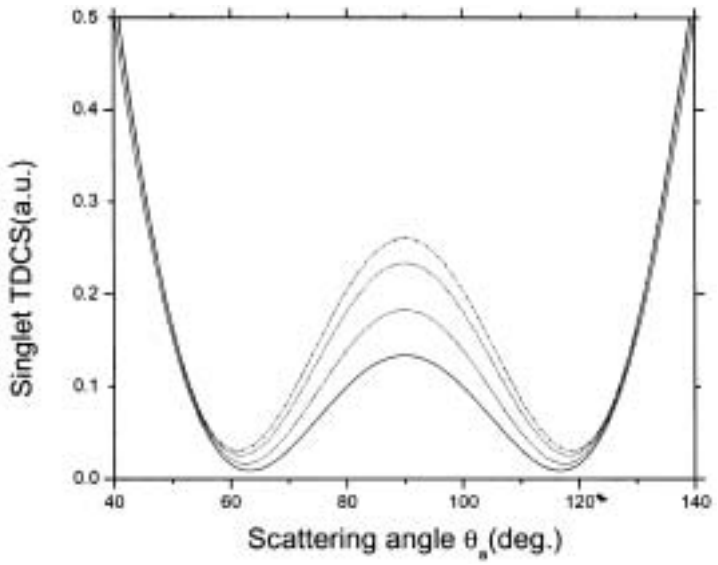

Figure 7. Singlet TDCS for electron impact ionization of hydrogen in equal energy sharing and $\vartheta_{ab} = 80^\circ$ kinematics as a function of scattering angle ϑ_a at excess energy $E_{\rm ex} = 0.5$ eV. Results: $E_{\rm ex} = 0.1$ eV (- ·· - ·· -), $E_{\rm ex} = 0.2$ eV (- - -), $E_{\rm ex} = 0.5$ eV (···), $E_{\rm ex} = 1.0$ eV (—).

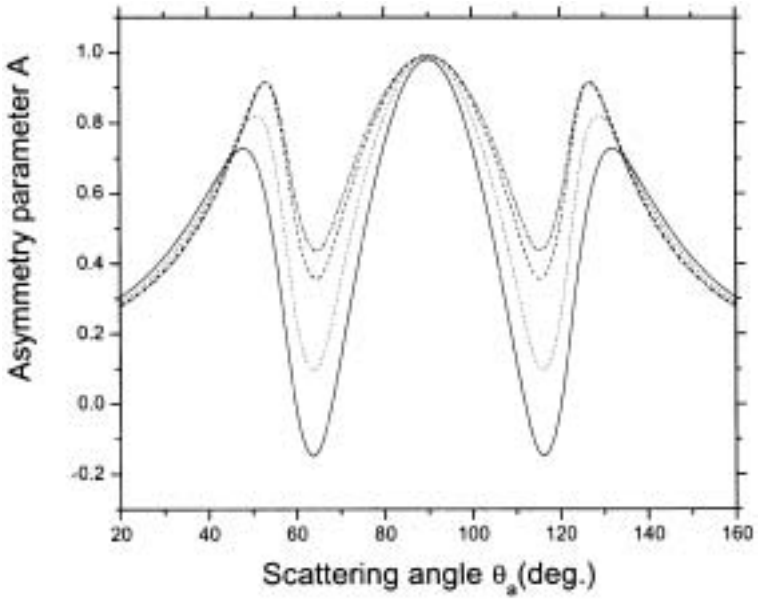

Figure 8. Asymmetry parameter A for electron impact ionization of hydrogen in equal energy sharing and $\vartheta_{ab} = 180^\circ$ kinematics as a function of scattering angle at various values of excess energy $E_{\rm ex}$. Results: $E_{\rm ex} = 0.1$ eV (- ·· - ·· -), $E_{\rm ex} = 0.2$ eV (- - -), $E_{\rm ex} = 0.5$ eV (···), $E_{\rm ex} = 1.0$ eV (—).

These are contributed by ^3P, ^3F,... and ^1S, ^1D,... partial waves respectively. The cross-section at $\vartheta_a = 90^\circ$ is contributed by singlet partial waves, but it does not necessarily lead to a maximum in TDCS at $\vartheta_a = 90^\circ$. This feature really depends on the relative magnitudes of the contributions of several partial waves. For example, at $E_{\rm ex} > 1.0$ eV, these contributions do not add up to a maximum at $\vartheta_a = 90^\circ$, while at lower values of $E_{\rm ex}$ they do. The contribution of the ^1D partial wave is most important. The maximum at $\vartheta_a = 90^\circ$ is essentially contributed by this partial wave. In the region around $\vartheta_a = 60^\circ$, the triplet cross-section decreases while the singlet cross-section increases with decreasing $E_{\rm ex}$.

Figure 8 shows the angular distribution of the asymmetry parameter A defined by

$$\begin{aligned} A &= (1-r)/(1+3r) \\ &= \mathrm{Re}(fg^*)/\left\lfloor |f|^2 + |g|^2 - \mathrm{Re}(fg^*)\right\rfloor , \end{aligned} \tag{13}$$

where $r = \sigma_T/\sigma_S$. It is identically equal to 1 at $\vartheta_a = 90^\circ$ where σ_T is zero. At excess energy $E_{\rm ex} = 1.0$ eV, the parameter A is negative in some angular region indicating that σ_T is greater than σ_S. At lower $E_{\rm ex}$, σ_S is always greater than σ_T and therefore its angular distribution effectively decides the angular distribution of the total TDCS.

4. Conclusions

The TDCS for the ionization of hydrogen at $E_{\rm ex} \leq 1.0$ eV in the equal energy sharing and $\vartheta_{ab} = 180°$ kinematics is found to decrease with increasing ϑ_a and shows a maximum at $\vartheta_a = 90°$ similar to the helium case close to threshold. This is found to become more pronounced as $E_{\rm ex}$ decreases. It is mainly contributed by the ^1D partial wave. However, its appearance depends on a critical balance between the singlet and triplet angular distributions. All these features are really determined by short range e–e correlations which dominate the cross-section at these low energies.

Acknowledgements

The Council of Scientific and Industrial Research, Government of India supported this work, under project No. 21(0497). RKC would like to thank the University Grants Commission for the award of a junior research fellowship.

References

[1] P Selles, A Huetz and J Mazeau, *J. Phys.* **B20**, 5195 (1987)
[2] P Schlemmer, T Rosel, K Jung and H Ehrhardt, *Phys. Rev. Lett.* **63**, 252 (1989)
[3] J Roder, H Ehrhardt, C Pan, A F Starace, I Bray and D V Fursa, *Phys. Rev. Lett.* **79**, 1666 (1997)
[4] P Selles, J Mezeau and A Huetz, *J. Phys.* **B23**, 2613 (1990)
[5] T Rosel, R Bar, K Jung and H Ehrhardt, *European Conf. on* $(e, 2e)$ *Collisions and Related Problems* edited by H Ehrhardt (Universitat Kaiserslautern, Kaiserslautern, Germany, 1989) pp. 69–81
[6] M Brauner, J S Briggs and H Klar, *J. Phys.* **B22**, 2265 (1989)
[7] M Brauner, J S Briggs and H Klar, *J. Phys.* **24**, 287 (1991)
[8] J Berakdar and J S Briggs, *Phys. Rev. Lett.* **72**, 3799 (1994)
[9] J Berakdar, *Phys. Rev.* **A56**, 370 (1997)
[10] Z Chen, Z Ni, Q Shi and K Xu, *J. Phys.* **B1**, 3803 (1998)
[11] S Jones and D H Madison, *Phys. Rev. Lett.* **81**, 2886 (1998)
[12] C Pan and A F Starace, *Phys. Rev. Lett.* **67**, 185 (1991)
[13] C Pan and A F Starace, *Phys. Rev.* **A45**, 4588 (1992)
[14] S Jones, D H Madison and M K Srivastava, *J. Phys.* **B25**, 1899 (1992)
[15] C Pan and A F Starace, *Phys. Rev.* **A47**, 2389 (1993)
[16] C T Whelan, R J Allan and H R J Walters, *J. Physique* **3**, 39 (1993)
[17] C T Whelan, R J Allan, R Rasch, H R J Walters, X Jhang, J Roder, K Jung and H Ehrhardt, *Phys. Rev.* **A50**, 4394 (1994)
[18] S Gupta and M K Srivastava, *J. Phys.* **B29**, 323 (1995)
[19] F Rouet, R J Tweed and J Langlois, *J. Phys.* **B29**, 1767 (1996)
[20] I Bray, D A Konovalov, I E McCarthy and A T Stelbovics, *Phys. Rev.* **A50**, R2818 (1994)
[21] I Bray, *J. Phys.* **B32**, L119 (1999)
[22] I Bray, *J. Phys.* **B33**, 581 (2000)
[23] C W McCurdy, T N Rescigno and D Byrum, *Phys. Rev.* **A56**, 1958 (1997)

[24] M Baertschy, T N Rescigno, W A Isaacs, X Li and C W McCurdy, *Phys. Rev.* **A63**, 022712 (2001)
[25] N C Deb and D S F Crothers, *J. Phys.* **B34**, 143 (2001)
[26] N C Deb and D S F Crothers, *Phys. Rev.* **A65**, 052721 (2002)
[27] J Roder, J Rasch, K Jung, C T Whelan, H Ehrhardt, R J Allan and H R J Walters, *Phys. Rev.* **A53**, 225 (1996)
[28] J B Furness and I E McCarthy, *J. Phys.* **B6**, 2280 (1973)
[29] F A Gianturco and S Scialla, *J. Phys.* **B20**, 3171 (1987)
[30] S Hara, *J. Phys. Soc. Jpn.* **22**, 710 (1967); **27**, 1009 (1969)
[31] M R H Rudge, *Rev. Mod. Phys.* **40**, 564 (1968)